Co-production of ethanol-hydrogen by genetically engineered *Escherichia coli* in sustainable biorefineries for lignocellulosic ethanol production

Angel Mario Lopez-Hidalgo[a,b,‡], Felicia Rodriguez[a,‡], Gabriela Magaña[a], Antonio De Leon-Rodriguez[b*], Arturo Sanchez[a*]

[a]Laboratorio de Futuros en Bioenergía, Unidad Guadalajara de Ingeniería Avanzada, Centro de Investigación y de Estudios Avanzados del Instituto Politécnico Nacional, Av. del Bosque 1145, Colonia el Bajío, Zapopan 45019, Jalisco, México

[b]División de Biología Molecular, Instituto Potosino de Investigación Científica y Tecnológica, Camino a la Presa San José 2055, Col. Lomas 4ª sec., C.P. 78216, San Luis Potosí, SLP., México.

[‡]Both authors contributed equally

Submitted to: *Chemical Engineering Journal*

[*]Corresponding authors.

E-mail addresses: arturo@gdl.cinvestav.mx (A. Sanchez)

aleonr@ipicyt.edu.mx (A. De Leon-Rodriguez)

Abstract

This work shows the impact of the hydrogen and ethanol co-production –via dark fermentation– using a genetically modified *Escherichia coli* in the environmental and economic sustainability of a lignocellulose-based biorefinery. Wheat straw (WS) and corn stover (CS) were used as feedstock pretreated with either a dilute acid pretreatment (DAP) or an autohydrolysis followed by very-dilute acid pretreatment (AH-VDAP) to compare the effect of the lignocellulosic matrix and the pretreatment as strategies for obtaining rich hemicellulosic hydrolysates, which were used as substrate in the dark fermentation experiments. Further, their impact on the profitability was determined on biorefinery conceptual designs incorporating the experimental results of the pretreatment and dark fermentation stages. The dark fermentation stage contributed with 20% to 30% of the total ethanol production in the lignocellulose-based biorefinery designs proposed in this work. Techno economic and sustainability analyses established that the biorefinery design using WS as feedstock and employing AH-VDAP presented the lowest negative environmental impact with the lowest Total Production Cost. The results show that co-production schemes could be an alternative for lignocellulosic ethanol biorefineries.

Keywords: lignocellulosic biomass; biorefineries; dark fermentation; metabolic engineering; techno economic analysis; sustainability analysis

1 Introduction

One of the most urgent and important challenges of this century is averting global warming whilst satisfying the growing energy demands of humankind. Renewable energies (*e.g.* solar, wind and biofuels) seems to be the most promising alternatives to address this challenge [1]. Therefore, the design, development, and optimisation of sustainable biorefineries for the efficient production of biofuels are needed to duly provide society with this renewable energy source [2,3]. A biorefinery is a facility in which biomass is converted into marketable products and energy using multistep processing approaches [4]. Lignocellulose is a sustainable and world-wide available biomass, thus a suitable feedstock for biorefining purposes [5,6]. Wheat straw (WS) and corn stover (CS) are lignocellulosic biomasses (LCB) with potential as feed-stocks for producing bioenergy and high value added products [7] since they are the most abundant agricultural residues worldwide. The annual global production of these residuals is around 0.5 and 1 billion tons, respectively [8,9]. Their glucan and xylan pools represents a significant potential source of glucose and xylose [10,11]. These carbohydrates, after being pretreated and hydrolysed [12], produce biofuels (*e.g.*, alcohols or hydrogen) by different fermentation strategies. Among them, dark fermentation has been extensively studied, concluding that high yields and productivities as well as low production costs are required to achieve profitable industrial-scale production [13–15]. Genetically modified microorganisms with redesigned metabolic systems have been hailed as a possible solution since they can improve yield and productivity, thus reducing CAPEX and OPEX [16–18]. In particular, *Escherichia coli* is the most convenient onset to engineering microbial catalysts for biofuel production owing to extensive knowledge of its genetic and metabolism [19,20]. Among those biofuels produced using microbial fermentation, hydrogen has gained interest because its eco-

friendly nature and energy content (120 kJ/g), as well as ethanol due to mature production technology and its well established existing fuel market [16,21]. *E. coli* is capable to co-produce hydrogen and ethanol through dark fermentation from pentoses and hexoses (analytical grade), as well as from hemicellulose hydrolisates? [22,23]. This is because oxidative decarboxylation of pyruvate to produce acetyl-CoA and formate. Therefore, the co-production of hydrogen and ethanol can be more profitable than their production in separate fermentation stages [24]. Moreover, co-production schemes can improve the energy balance of the biorefinery designs [25,26].

This work studies the impact of hydrogen and ethanol co-production from hemicellulose – via dark fermentation– using a genetically modified *E. coli* strain in the sustainability of a biorefinery producing ethanol and hydrogen using lignocellulosic biomass. Two types of lignocellulosic biomass, which were subject to two different pretreatment methods to obtain hemicellulose-rich hydrolysates, and then used in the dark fermentation as substrate. Results were used for designing of biorefineries employing the dark-fermentation stage for improving the biorefinery energy balance. This stage provided part of the ethanol produced in the biorefinery, as well as the hydrogen used together with the biogas and solid residues from the wastewater treatment stage for cogenerating energy. The dark fermentation batches were carried out with hemicellulosic hydrolysates from WS and CS obtained from dilute acid pretreatment (DAP) or autohydrolysis followed by very-dilute acid pretreatment (AH-VDAP). These pretreatment methods were selected based on their glucose and hemicellulose high yields obtained in post-pretreatment stages from previous experiences on pilot-scale continuous mode pretreatment strategies [10,11,27] and their high yield in hydrogen production [28,29]. Techno economic and sustainability analyses of the resulting biorefinery designs was carried out considering the environmental and economic domains

[30] to identified the role of the co-production of hydrogen and ethanol strategy on the proposed biorefinery designs.

2 Experimental setup and procedures

2.1 Feedstocks

Wheat straw (WS) and corn stover (CS) were harvested in the spring of 2017 in La Barca (Jalisco, Mexico). Both feedstocks were milled with a hammer mill (Azteca 301012) using a 1.27 cm screen. LCB composition was determined according to NREL analytical procedures [31]. Cellulose, hemicellulose, and lignin content in LCB (dry basis) were 48.88, 17.83 and 6.51% for WS; and 43.00, 22.11 and 18.00% for CS, respectively.

2.2 LCB pretreatment methods

Hemicellulosic hydrolysates were produced by two methods: a) dilute acid pretreatment (DAP) and b) autohydrolysis followed by a very-dilute acid pretreatment (AH-VDAP). DAP was carried out in an autoclave at 121°C for 1 hour with a 15% (w/v) solid loading and 1.5% (v/v) H_2SO_4. Liquid fractions from DAP using WS and CS as feedstock were identified as WSC and CSC, respectively. Autohydrolysis (AH) was carried out in a semi-pilot scale pretreatment continuous tubular reactor (PCTR) at 1034 kPa (185°C) with a mean residence time of 18 min [11]. Pretreated biomass from AH was further hydrolysed in an autoclave at 121°C for 60 min using H_2SO_4 0.25% (v/v) with a 1:2 (w/v) ratio solids loading. Liquid fractions from AH-VDAP using wheat straw and corn stover as feedstock were identified as WSP and CSP, respectively. The hydrolysates composition is shown in Table 1. Further hydrolysates dilutions were made to obtain concentration between 10-15

g/L of total reducing sugars, which were used in the experiments of co-production of hydrogen and ethanol via dark fermentation described in the following subsection.

2.3 Hydrogen and ethanol co-production via dark fermentation by the genetically modified *E. coli* strain

The genetically modified *E. coli* strain used in this work has a genotype that corresponds to absence of *hycA, ldhA* and *frdD* genes. These genes were deleted as described elsewhere [32]. This genotype confers the strain the ability to overproduce ethanol (EtOH) and hydrogen (H_2), as well as decreasing the amounts of lactic and succinic acids produced. From now on, this strain will be referred as EtOH-H_2-coproducing *E. coli*. The co-production of hydrogen and ethanol was performed using hemicellulosic hydrolysates as substrates, at 31°C and initial pH of 8.2. Diluted WSC, CSC, WSP, and CSP were used to determine the effect of LCB pretreatment method on the co-production of hydrogen and ethanol by the coproducing *E. coli*. These experiments were carried out in anaerobic serological bottles (0.01 L working volume) containing 10-15 g/L of total reducing sugars, B buffer [33], 1 mL/L trace elements solution [34], 0.01 g/L $MgSO_4$ and 1 g/L yeast extract. Cultures were started with an optical density of 0.2 measured at a wavelength of 600 nm and were shaken at 200 rpm until no generation of hydrogen was observed. The experiments were carried out in quadruplicate. Production of hydrogen and ethanol was measured as it is indicated in Section 2.4.

2.4 Analytical methods

Total reducing sugars (TRS) was determined by the dinitrosalicylic acid (DNS) method [35], with some modifications as follows: 250 µL of the diluted sample with 750 µL of

DNS reagent (10 g/L NaOH, 200 g/L $KNaC_4H_4O_6 \cdot 4H_2O$, 0.5 g/L $Na_2S_2O_5$, 2 g/l C_6H_6O, 10 g/L 3,5-Dinitrosalicylic acid) were heated for 5 minutes at 100ºC and then cooled down to room temperature. Once tempered, 400 µL of distilled water were added. Xylose (0.1 to 1.0 g/L) was used as the reference standard. The absorbance was measured at 595 nm (iMark™ Microplate Absorbance Reader).

Simple sugars and metabolites were quantified by an Agilent HPLC equipped with a refractive index detector (Agilent Technologies 1220 Infinity LC), using a Rezex™ ROA-Organic Acid H+ (Phenomenex) column, operated at 60°C with H_2SO_4 0.0025 M as a mobile phase (0.50 mL/min). Furfural was analysed by gas chromatography (Agilent Technologies 6890N Network GC Systems) using a capillary column HP-Innowax (30 m length × 0.25 mm inner diameter × 0.25 µm film thickness; Agilent Technologies). Injector and flame ionization detector (FID) temperatures were 220 and 250 °C, respectively. Helium was used as carrier gas at a flow rate of 25 cm^3/min. Analyses were performed with a split ratio of 10:1 and a temperature program of 35 °C for 2 min, then 10°C/min to 210°C for 1 min.

Gas production was measured by acidified water (pH ≤ 2) displacement in an inverted burette connected to serological bottles with rubber tubing and a needle. The hydrogen concentration (%, v/v) in the gas phase was determined by gas chromatography with a thermal conductivity detector (Agilent Technologies 6890N Network GC Systems) using an Agilent J&W HP-PLOT Molesieve column (30 m length × 0.32 mm inner diameter × 12 µm film thickness) under the following conditions: 200°C, injector temperature; 280°C, detector temperature; 300°C, oven temperature. Helium was used as carrier gas. Hydrogen volume was corrected to standard conditions of temperature and pressure (298.15K and 10^5 Pa).

3 Modelling and simulation

3.1 Process description of the biorefinery design

Biorefining schemes were designed to produce ethanol from lignocellulosic biomass. All schemes are similar, differing only in the feedstock (WS or CS) and pretreatment method (DAP or AH-VDAP). Fig. 1 shows a block diagram of the proposed biorefinery conceptual design co-producing ethanol and hydrogen using WS or CS as feedstocks with an installed capacity of 500-ton biomass/day. Biogas produced from biorefining residues, hydrogen, lignin, and fermentation residues are used in a co-generation stage for steam and electricity production. The biorefineries designs were based on the models previously described elsewhere [30,36], with the following particularities:

a) DAP or AH-VDAP were applied as pretreatment methods of LCB to obtain hemicellulosic hydrolysates (see description on Section 2.2).
b) Hemicellulosic hydrolysates from the pretreatment stage (see description on Section 2.3) were used as substrate by the EtOH-H_2-coproducing *E. coli* strain. In the biorefinery designs, this stage provided part of the total production of ethanol, as well as the hydrogen used in the cogeneration stage.

The biorefinery designs evaluated were termed WSB1, WSB2, CSB1 and CSB2 (WSB: biorefineries using wheat straw as feedstock; CSB: biorefineries with corn stover as feedstock; 1: DAP as pretreatment method; 2: AH-VDAP as pretreatment method). Each design was composed by a traditional lignocellulosic ethanol production train [feedstock conditioning (feedstock cleaning and size reduction), pretreatment (DAP or AH-VDAP), enzymatic saccharification, alcoholic fermentation, separation (azeotropic distillation and molecular sieving)], a dark fermentation (hydrogen and ethanol co-production) stage, a

wastewater treatment (anaerobic treatment, aerobic treatment and clarification) plant, and a cogeneration (steam and electricity) stage. The process inputs for each designs were raw materials (H_2SO_4, $Ca(OH)_2$, enzymes, yeasts, bacteria, *E. coli* WDH-LF, flocculants, and antifoams), utilities (fresh water, pressurized air, electricity, steam-generator fuel) and the feedstock (WS or CS). The outputs were energy (electricity), steam, wastes (water, CO_2, ashes, cake, and other solid wastes) and ethanol as product. Biorefineries mass and energy steady state balances were implemented in continuous mode and solved using the SuperPro Designer v8.5 (SPD) simulator [37]. Process conditions and reactions rates for pretreatment and dark fermentation stages correspond to the experimental data obtained as described in Sections 2.2 and 2.3. Integration of energy and 20% of water recirculation to the process were considered. Process details are provided in the Supporting Information.

3.2 Techno economic analysis

The profitability of each biorefinery design proposed in the section above was analysed with techno economic analysis tools previously implemented and tested with similar designs to those proposed in this work [38,39]. The analysis was based on the Discounted Cash Flow Analysis (DCFA) method for Net Present Value (*NPV*) = 0 [40], calculating total capital investment, total production cost (*TPC*), and their contributions for all biorefinery designs. The biorefinery energy integration was carried out using the Pinch Point Analysis technique for maximum energy recovery [40]. The End Use Energy Ratio (*EER*) was employed to evaluate the energy efficiency of each design. *EER* was defined as ratio of energy produced (steam, electricity, and chemical energy from ethanol) to the total energy consumed in the process (heating/cooling requirements and electricity) [41]. Equipment size and cost were calculated based on plant capacity using the SPD economic

data-base and its construction material and capacity-based correlations. All costs and financial parameters corresponded to conditions (c. 2018) of the Mexican economy. Commissioning and plant life periods were fixed at 3 and 15 years, respectively, with 330 operating days/year. The interest rate was set at 6% and equity at 30%. Full production was assumed to begin by the end biorefinery's commissioning.

3.3 Sustainability analysis

A sustainability analysis method –previously developed for assessing prospective biorefining technologies [30]– was employed to quantify the impact of the biorefinery designs in the environmental and economic domains. Where, those impacts are calculated with quantitative indicators for each domain. Each indicator is integrated by one or more metrics related to design and/or process variables of the biorefinery design in question. Table 2 shows the indicators and metrics to be evaluated for each domain (based on the sustainability framework previously used for similar evaluations [36,38]). Six indicators are part of the environmental domain whilst two indicators were defined for the economic counterpart. All metrics (environmental and economic) are translated to the same functional unit using ad-hoc dimensional functions and conversion coefficients that are defined based on regulatory frameworks where the biorefinery facilities would be located. In this study, the functional unit chosen was USD/MJ_{out} to monetize the impacts per of unit of energy delivered by the biorefinery. The translation of metric values to the same functional unit was obtained applying the following equation

$$\eta_i = M_i \cdot C_i,$$

Where η_i is the monetized metric i; M_i the metric value, and C_i the monetizing coefficient (*i.e.* conversion). In addition, signs were assigned to each metric according to its positive or

234 negative impact to the corresponding domain. A positive value is associated to a benefit
235 received by the stakeholders, whilst a negative value might be interpreted as a cost that
236 stakeholders must cover. Table 3 contains the metric values, as well as monetizing
237 coefficients and their corresponding monetized values (USD/MJ_{out}). One of them, the
238 *Emitted GHG* indicator, or "carbon intensity" with its associated metric was calculated as
239 the carbon dioxide produced during the fermentation processes and electricity cogeneration
240 stages. The monetization considers an impact cost of $123 USD per metric ton of CO_2 [42].
241 This cost includes the damage caused to water resources, land and biodiversity, agriculture
242 and forestry, ecosystems, and human health. The *Emitted non-GHG* indicator, whose metric
243 is composed by SO_2 emissions in the electricity generation stage, was monetized using the
244 trading value of SO_2 in the US Acid Rain Program [43]. *Water consumption* and
245 *Wastewater quality* indicators were monetized according to current Mexican environmental
246 regulations [44,45]. These indicators are formed by more than one metric (Table 2).
247 Therefore, their monetized value is the sum of their monetized metrics. The *Amount of*
248 *produced solid wastes* indicator was monetized using the cost of solid waste management
249 services in Mexico, which is $76.89 USD per ton of waste transferred and disposed [46].
250 As was described in Section 3.2, the *EER* indicator is the ratio of energy produced to the
251 total energy consumed in the process. In the economic domain, two indicators were
252 considered: *TPC* and *Electrical productivity*. The *TPC* indicator was monetized by
253 translating all products to their energy equivalents. Finally, the *Electrical productivity*
254 indicator was monetizing using the cost per MJ of electricity produced as a fraction of the
255 total energy generated by the biorefinery [37].
256 Sustainability indicators per domain are calculated by adding their corresponding
257 indicators. The "global sustainability value" is the sum of all the environmental and

economic indicators once they are monetized. For a comparative analysis of the impact of each indicator in the biorefinery designs, all metric values were normalized with respect to WSB1 design considered the base case.

4 Results and discussion

4.1 LCB pretreatment methods

The characterization of hemicellulosic hydrolysates (hemicellulose to pentoses conversion, composition of simple sugars, degradation compounds) from pretreatment is shown in Table 1. As expected, xylose was the highest concentration sugar monomer in the hydrolysates obtained with both LCB pretreatment methods. DAP decomposed hemicellulose while maintained cellulose and lignin almost intact [27,47]. WSC and CSC produced 29 and 34.3 g/L of xylose, respectively. Regarding AH-VDAP, the xylan backbone was selectively depolymerized during autohydrolysis, resulting into xylooligosaccharides (XOS) as main reaction products [48]. These XOS were depolymerized during the subsequent very-diluted acid pretreatment stage, resulting in large concentrations of xylose at the end of the pretreatment. WSP and CSP generated 39.8 and 41.1 g/L of xylose, respectively. Glucose concentrations in WSP and CSP were 3-fold less than in WSC and CSC hydrolysates (Table 1) since the glucan of LCB biomass was not depolymerized during autohydrolysis as reported previously [11], and the sulphuric acid concentration of very-diluted acid pretreatment stage was chosen for depolymerizing XOS.

The aims of pretreatment are to disrupt the crystalline cellulose structure and to fractionate the main components of the feedstock [49]. However, during pretreatment of LCB, by-products are often produced that can inhibit downstream biochemical processes. These inhibitors are formed when hemicellulose, cellulose and/or lignin are solubilized and

degraded [50,51]. Acetate was the main pretreatment by-product found in all hydrolysates, followed by formate and furfural. Acetate results from the hydrolysis of acetyl groups of hemicelluloses [52], and it was detected in concentrations higher than 4 g/L (Table 1). Even though acetate, formate and furfural have relatively low toxicity [50], to avoid their possible inhibiting effects in dark fermentation experiments, the hydrolysates were diluted with water. After dilution, the concentration of total reducing sugars was 15.1, 9.7, 10.2 and 11.1 g/L in WSC, WSP, CSC and CSP, respectively.

4.2 Dark fermentation by the EtOH-H2-coproducing *E. coli* strain

The effect of DAP and AH-VDAP hydrolysates on the EtOH-H_2-coproducing *E. coli* are shown in Fig. 2. Using WSC as substrate up to 1.3-fold more hydrogen was obtained than with WSP (Fig. 2A). This is because of the difference of TRS concentration among hydrolysates after dilution, with WSC having 1.6-fold more TRS than WSP. Similar event was observed using CSC or CSP as substrates. With a TRS concentration in CSP 1.1-fold higher than in CSC, CSP produced 2,930.3 ± 189.4 mL H_2/L whilst CSC reached 2,576.4 ± 220.4 mL H_2/L. Regarding hydrogen production rate, 22.1 ± 1.1, 18.3 ± 1.0, 20.2 ± 1.7 and 18.5 ± 1.3 mL H_2/L·h were obtained using WSC, WSP, CSC and CSP as substrate, respectively. Note that production rates were higher with DAP hydrolysates than with the AH-VDAP counterparts. Hydrogen production kinetics and the percentage of hydrogen in the gas attained by the EtOH-H_2-coproducing *E. coli* are showed in Fig. 3. None of the batches presented lag phase since hydrogen was found from the first gas sampling (17 h). The maximum concentration of hydrogen (%, v/v) in the gas phase detected was 56% (at 17 h, WSC), 45% (at 40 h, WSP), 46% (at 40 h, CSC) and 50.2% (at 40 h, CSP). Hydrogen production declined after 120 h of fermentation, regardless of the kind of feedstock and

type of pretreatment used. Fig. 2B shows the hydrogen yield and TRS consumption by the EtOH-H_2-coproducing *E. coli* strain. The TRS consumption was 10% higher using WSP as substrate than with WSC. However, this was not observed with CSC or CSP. The yield of hydrogen achieved by EtOH-H_2-coproducing strain was 311.5 ± 30.7, 323.1 ± 6.6, 312.3 ± 26.7 and 337.1 ± 21.8 mL H_2/g TRS using WSC, WSP, CSC and CSP as substrate, respectively. Regarding ethanol production (Fig. 2C), up to 3.54 ± 0.27 g/L were produced at the end of fermentation, achieving yields in the range of 0.32 ± 0.01 to 0.34 ± 0.06 g EtOH/g TRS (for all hydrolysates). Therefore, amount of ethanol produced per TRS unit seems to be not affected by feedstock or pretreatment method.

The co-production of hydrogen and ethanol by microorganisms had been studied using genetically engineered *E. coli* strains. Different molecular strategies had been tested to enhance the fermentation efficiency of *E. coli* strains, such as deletion of genes including those to produce hydrogenases, negative regulator of the formate regulon, lactate dehydrogenase, fumarate reductase and phosphoglucose isomerase, among other [20,25,26,53], as well as heterologous gene expression [54]. Many of these studies used glucose as carbon source instead of LCB hydrolysates. Interestingly, reported hydrogen and ethanol yields are lower than those obtained in this work (Table 4). In previous studies, whet straw hydrolysate was used as substrate for co-production hydrogen and ethanol by metabolic engineered *E. coli* strains, WDHL [22] and WDHGFA [23]. Reported yields of hydrogen and ethanol obtained by WDHL strain were 159 mL H_2/g sugar and 0.32 g EtOH/g sugar, while WDHGFA strain reached 160 mL H_2/g sugar and 0.26 g EtOH/g sugar. These amounts are either similar or lower up to 47% than those obtained here as seen in Table 4.

Since the aim of this work was to improve the lignocellulosic ethanol biorefinery performance by co-producing hydrogen and ethanol by genetically modified *E. coli*, the experimental data provided above was included in the conceptual design of (environmental and economic) sustainable biorefineries, as described in the following subsections.

4.3 Mass balances

As mentioned previously, DAP and AH-VDAP of WS and CS were included as pretreatment methods to compare their effect on the dark fermentation performance and therefore on the biorefinery economics. The process schemes evaluated were WSB1, WSB2, CSB1 and CSB2 (see Section 3.1 for a detail description). The mass balances for the stages involved in ethanol production for all biorefineries are shown in Figs. 4 and 5. For mass conversion ($X_{A \rightarrow B}$) data see Tables A1, A2 and A3 in the Supporting Information. Table 5 shows output flowrates from each of the biorefining stages. CSB1 and CSB2 produced 4,825 and 4,912 kg/h of pentoses in the pretreatment stage, 24% more than WSB1 and WSB2. This is because hemicellulose fractions in CS are 1.2-fold higher than in WS, as well as the $X_{Hemic. \rightarrow Pentoses}$ during the pretreatment stage in CSB1 and CSB2 is 7% and 5% higher than in WSB1 and WSB2, respectively.

In the dark fermentation stage, the hemicellulosic hydrolysates from the pretreatment stage were used by the EtOH-H2-coproducing *E. coli* strain to obtain hydrogen and ethanol. WSB1, WSB2, CSB1 and CSB2 produced 26.3, 25.1, 44.1 and 45.8 kg/h of hydrogen, respectively, which were fed to the cogeneration stage for electricity production. The difference in hydrogen production among schemes is due to a smaller $X_{Sugars \rightarrow H_2}$ (15%) and the lower hemicellulose fraction for WS (Table 5). Regarding ethanol, WSB1, WSB2,

CSB1 and CSB2 produced 6,093, 6,126, 5,742 and 5,796 kg/h of ethanol, respectively. Around 20-30% of this comes from dark fermentation, and the rest from alcoholic fermentation (Table 5). Since WS presented the highest cellulose content, WS-based biorefineries produces 6% more ethanol than CS-based counterparts.

4.4 Techno economic analysis results

After establishing the contribution of dark fermentation over ethanol production in the proposed conceptual designs, their profitability was determined by a techno economic analysis considering Mexican economic conditions (c. 2018). The total equipment cost is 10.1%, 46.8% and 22.2% higher in WSB1, CSB1 and CSB2 compare to WSB2, respectively (Fig. 6A). The equipment cost per stage, as shown in Fig 6B, is similar in all cases, except for the pretreatment and dark fermentation stages. On one hand, CS-based biorefineries have the most expensive dark fermentation stage ($57-58 USD millions) due to the higher amount of pentoses obtained from the pretreatment stage than with WS. Therefore, a larger amount of water is needed to achieve the sugars concentration required in the dark fermentation stage. As a consequence, higher volume reactors must be employed with larger costs. On the other hand, the pretreatment stage equipment cost of AH-VDAP biorefineries (WSB2 and CSB2) is about 60 % lower than their DAP counterparts since a continuous reactor was considered for this case.

Fig. 7 shows the TPC calculated per litre of ethanol for each biorefining design, as well as their ethanol production. The lowest *TPC* ($1.37 UDS/L EtOH, Fig. 7A) was obtained by WSB2, which is 17.9, 43.1 and 15.9% lower than those obtained for WSB1, CSB1 and CSB2, respectively. Even when WS is 2.5-fold more expensive than CS (Table 1), feedstock cost seems not to contribute to *TPC* in that proportion. WS seems to be a better

feedstock for ethanol production compared to CS due to its higher cellulose content. The most important contributors to *TPC*, as shown in Fig. 7B, are operation cost followed by services (cooling and heating) and total capital investment, with values around 29.8-34.7%, 14.5-22.4% and 15.4-18.3%, respectively. Operating cost include maintenance, operating supplies, labour, and direct supervision, laboratory charges, patents, and royalties. Regarding the services contribution to *TPC*, the highest values were corresponding to those designs using DAP pretreatment since a higher amount of cooling water is required by the process during pretreatment stage. Electricity consumption is not a relevant contributor to *TPC*. Electricity demand ($Electricity_{in}$) of all biorefineries is more than 5,800 kWh of electricity (Fig. 8). However, they produce ($Electricity_{out}$) just around 20-30% of this demand, thus *EER* is lower than 0.50 for all designs. WSB2 is the most economical option, because it produces the largest amount of ethanol with the lowest equipment cost.

4.5 Sustainability analysis results

4.5.1 Environmental Sustainability Analysis Results

The results of the sustainability analysis for the environmental domain are summarized in Table 3. Once monetized, all indicators were of negative value, with the *EER* indicator as the main contributor in this domain, with a contribution of more than 67% of the *Total Environmental Indicator* for all designs. The electricity dependence has been observed in the analysis of other biorefinery designs producing biofuels as the main product [30]. Other important indicator is *EGHG* with a contribution of around 15-21%. *WCo* and *WWQ* indicators provide a contribution about ≤7% for all cases because the biorefinery was designed for water recirculation and for complying with the Mexican regulatory framework

for discharges to water bodies [44]. *SW* indicator is the lowest contributor with ≤ 3.7% for all cases.

To compare the environmental indicators performance among biorefineries, metric values were normalized with respect to WSB1 (base case) as shown in Fig. 9. *T* and *pH* metrics were not included because they are similar in all cases. For M_{CO2} –which is related to GHG emission generated during dark fermentation, alcoholic fermentation and cogeneration stages–, CS-based biorefineries produced around 22-25% more g CO_{2eq} per MJ than the base case since a higher amount of lignin, H_2 and biogas are fed to the cogeneration stage which is the main contributor to this metric and therefore to GHG emissions indicator. In the case of M_{SO2}, the only non-greenhouse gas considered in this work is SO_2, produced during the cogeneration stage due to sulphur contained in LCB. Corn stover (CSB1 and CSB2) biorefineries emitted 20% and 28% less g SO_{2eq} by MJ produced than the base case, respectively. This is principally due to differences in feedstocks composition. Regarding water consumption (M_{fw}), CS-based biorefineries employ around 26-39% more water than their WS-based counterparts. This is because the water required adjusting TRS in the pretreatment output stream feeding the dark fermentation stage. Discharged water (M_{dw}, $L_{discharged\ water}/MJ_{out}$) by WSB1 was 36, 30 and 73% lower than WSB2, CSB1 and CSB2, respectively. For the *WWQ* indicator, the metrics M_{COD} and M_{dp} –which are related to organic material and other pollutants content in wastewater treated– are lower in CSB1 and CSB2 than in WS-based biorefineries, because CSB1 and CSB2 streams are more diluted than those for the other two designs. The metric (M_{sw}) of *SW* indicator is directly related to solids generated by *pH* adjustment, as well as ash production in the cogeneration stage and dust from the conditioning stage. The *pH* in the dark fermentation stage by EtOH-H_2-

coproducing *E. coli* is 8.2. Therefore, the hydrolysates coming from the DAP-based biorefineries (WSB1 and CSB1) demand larger $Ca(OH)_2$ amounts than their counterparts, thus producing 89 and 77% more solid wastes than WSB2 and CSB2, respectively. Regarding energy self-sufficiency, WSB2 is the biorefinery with the highest *EER* value (0.49) because is the biorefinery with the largest ethanol production, surpassing in 12% the base scheme (Fig. 9). However, none of the biorefinery designs was energetically self-sufficient.

4.5.2 Economic Sustainability Analysis Results

The results of the sustainability analysis for the economic domain are presented in Table 3. After monetization, *TPC* is the most relevant indicator, with a 99% contribution for all cases. Therefore, WSB2 is the best alternative in the economic domain due to its lowest *TPC*. The indicator normalization using WSB1 as base case is shown in Fig. 10. WSB2 exhibited the lowest *TPC* (Fig. 7A), due to the lowest total equipment investment and highest ethanol production (Figs. 6A, 7A) as explained in Section 4.4. CSB1 and CSB2 exhibited the highest electrical productivity, surpassing in 60% and 46% the base case, respectively. Since the contribution of this indicator to the economic sustainability indicator is $\leq$1%, its impact is not relevant in the *Total Economic Indicator*.

4.5.3 Global Sustainability Analysis Results

The indicator values for each domain together with the global sustainability indicator are shown in Fig. 11. These values represent what stakeholders should pay per each MJ produced for either fines, and environmental damages caused by the biorefinery regarding the environmental domain or production costs considering the economic domain. From an

environmental point of view, the lowest impact is associated with WSB2, (-0.047 USD/MJ_{out}) since its *EER* indicator (positive) was the highest, as well as *EGHG* and *SW* (negative) indicators were the lowest values of all designs. The absolute value of this indicator is 26, 69 and 48% lower than those calculated for WSB1, CSB1 and CSB2, respectively. From an economic perspective, WSB2, again, achieved the lowest value of the four proposed schemes, with -0.064 USD per MJ produced, mainly due to its lowest *TPC*. Further, considering the *Global Sustainability Indicator*, the smallest value of all biorefinery scenarios is -0.111 USD per MJ produced, associated to WSB2. 43% of its value corresponds to the *Total Environmental Indicator*, and the rest to the *Total Economic Indicator*. The second-best option is WSB1, with a global impact value 23% higher than that for WSB2.

5 Conclusions

The dark fermentation stage –by EtOH-H2-coproducing *E. coli*– contributes with 20 to 30% of the total ethanol production in the lignocellulose-based biorefinery designs is proposed in this work. From all designs, WSB2 (wheat straw as feedstock and AH-VDAP as LCB pretreatment method) could generate the smallest environmental impact with the lowest *TPC*, which is up to 43% lower than its counterparts. The sustainability analysis shows the importance of environmental issues compared against economic aspects, fact that is not evident using conventional techno economic analysis tools. Based on the regulatory framework employed, the environmental monetized impact of the most sustainable design resulted almost as important as the economic aspects of it. Therefore, the results show that co-production schemes are an alternative for ethanol biorefineries that must be explored further.

Acknowledgements

Financial support is kindly acknowledged from the Energy Sustainability Fund 2014-05 (CONACYT-SENER), Mexican Bioenergy Innovation Center, Bioalcohols Cluster (Grant No.249564). A. Lopez-Hidalgo thanks the National Council of Science and Technology (CONACYT) for his postdoctoral fellowship 385574.

References

[1] International Energy Agency, World Energy Outlook 2019, OECD, Paris, 2019. https://www.iea.org/reports/world-energy-outlook-2019.

[2] A. Santangeli, T. Toivonen, F.M. Pouzols, M. Pogson, A. Hastings, P. Smith, A. Moilanen, Global change synergies and trade-offs between renewable energy and biodiversity, GCB Bioenergy. 8 (2016) 941–951. https://doi.org/10.1111/gcbb.12299.

[3] J. Teter, P. Le Feuvre, M. Gorner, S. Scheffer, Tracking Transport, Int. Energy Agency, Reports. (2019). https://www.iea.org/reports/tracking-transport-2019/transport-biofuels.

[4] E. de Jong, G. Jungmeier, Biorefinery Concepts in Comparison to Petrochemical Refineries, in: A. Pandey, R. Höfer, M. Taherzadeh, K.M. Nampoothiri, C. Larroche (Eds.), Ind. Biorefineries White Biotechnol., Elsevier B.V., 2015: pp. 3–33. https://doi.org/10.1016/B978-0-444-63453-5.00001-X.

[5] M. Villegas Calvo, B. Colombo, L. Corno, G. Eisele, C. Cosentino, G. Papa, B.

493 Scaglia, R. Pilu, B. Simmons, F. Adani, Bioconversion of Giant Cane for Integrated
494 Production of Biohydrogen, Carboxylic Acids, and Polyhydroxyalkanoates (PHAs)
495 in a Multistage Biorefinery Approach, ACS Sustain. Chem. Eng. 6 (2018) 15361–
496 15373. https://doi.org/10.1021/acssuschemeng.8b03794.
497 [6] J.A. Melero, J. Iglesias, A. Garcia, Biomass as renewable feedstock in standard
498 refinery units. Feasibility, opportunities and challenges, Energy Environ. Sci. 5
499 (2012) 7393–7420. https://doi.org/10.1039/c2ee21231e.
500 [7] F. Cherubini, The biorefinery concept : Using biomass instead of oil for producing
501 energy and chemicals, Energy Convers. Manag. 51 (2010) 1412–1421.
502 https://doi.org/10.1016/j.enconman.2010.01.015.
503 [8] M. Kapoor, D. Panwar, G.S. Kaira, Bioprocesses for Enzyme Production Using
504 Agro-Industrial Wastes: Technical Challenges and Commercialization Potential, in:
505 G.S. Dhillon, S. Kaur (Eds.), Agro-Industrial Wastes as Feed. Enzym. Prod. Apply
506 Exploit Emerg. Valuab. Use Options Waste Biomass, Elsevier Inc., 2016: pp. 61–93.
507 https://doi.org/10.1016/B978-0-12-802392-1.00003-4.
508 [9] Z. Ruan, X. Wang, Y. Liu, W. Liao, Corn, in: Z. Pan, R. Zhang, S. Zicari (Eds.),
509 Integr. Process. Technol. Food Agric. By-Products, Elsevier Inc., 2019: pp. 59–72.
510 https://doi.org/10.1016/b978-0-12-814138-0.00003-4.
511 [10] J.A. Pérez Pimienta, G. Papa, A. Rodriguez, C.A. Barcelos, L. Liang, V. Stavila, A.
512 Sanchez, J.M. Gladden, B.A. Simmons, Pilot-scale hydrothermal pretreatment and
513 optimized saccharification enables bisabolene production from multiple feedstocks,
514 Green Chem. 21 (2019) 3152–3164. https://doi.org/10.1039/c9gc00323a.
515 [11] F. Rodríguez, L. Amaya-Delgado, A. Sanchez, Xyloligosacharides production from
516 lignocellulosic biomass using a pretreatment continuous tubular reactor. Modelling

and experimental validation., Ind. Crop. Prod. 134 (2019) 62–70. https://doi.org/10.1016/j.indcrop.2019.03.058.

[12] P. Tsafrakidou, A. Bekatorou, A.A. Koutinas, C. Kordulis, I.M. Banat, T. Petsi, M. Sotiriou, Acidogenic Fermentation of Wheat Straw After Chemical and Microbial Pretreatment for Biofuel Applications, Energy Convers. Manag. 160 (2018) 509–517. https://doi.org/10.1016/j.enconman.2018.01.046.

[13] L. Wang, S.W. York, L.O. Ingram, K.T. Shanmugam, Simultaneous fermentation of biomass-derived sugars to ethanol by a co-culture of an engineered Escherichia coli and Saccharomyces cerevisiae, Bioresour. Technol. 273 (2019) 269–276. https://doi.org/10.1016/j.biortech.2018.11.016.

[14] W. Ye, J. Li, R. Han, G. Xu, J. Dong, Y. Ni, Engineering coenzyme A-dependent pathway from Clostridium saccharobutylicum in Escherichia coli for butanol production, Bioresour. Technol. 235 (2017) 140–148. https://doi.org/10.1016/j.biortech.2017.03.085.

[15] J.R. Bastidas-Oyanedel, F. Bonk, M.H. Thomsen, J.E. Schmidt, Dark fermentation biorefinery in the present and future (bio)chemical industry, Rev. Environ. Sci. Biotechnol. 14 (2015) 473–498. https://doi.org/10.1007/s11157-015-9369-3.

[16] J.C. Liao, L. Mi, S. Pontrelli, S. Luo, Fuelling the future: Microbial engineering for the production of sustainable biofuels, Nat. Rev. Microbiol. 14 (2016) 288–304. https://doi.org/10.1038/nrmicro.2016.32.

[17] A.J. Shaw, F.H. Lam, M. Hamilton, A. Consiglio, K. MacEwen, E.E. Brevnova, E. Greenhagen, W.G. LaTouf, C.R. South, H. van Dijken, G. Stephanopoulos, Metabolic engineering of microbial competitive advantage for industrial fermentation processes, Science (80-.). 353 (2016) 583–586.

https://doi.org/10.1126/science.aaf6159.

[18] P.E.P. Koskinen, S.R. Beck, J. Örlygsson, J.A. Puhakka, Ethanol and hydrogen production by two thermophilic, anaerobic bacteria isolated from Icelandic geothermal areas, Biotechnol. Bioeng. 101 (2008) 679–690. https://doi.org/10.1002/bit.21942.

[19] T. Liu, C. Khosla, Genetic Engineering of Escherichia coli for Biofuel Production, Annu. Rev. Genet. 44 (2010) 53–69. https://doi.org/10.1146/annurev-genet-102209-163440.

[20] T. Maeda, V. Sanchez-Torres, T.K. Wood, Hydrogen production by recombinant Escherichia coli strains, Microb. Biotechnol. 5 (2012) 214–225. https://doi.org/10.1111/j.1751-7915.2011.00282.x.

[21] P. Sivagurunathan, C. Kuppam, A. Mudhoo, G.D. Saratale, A. Kadier, G. Zhen, L. Chatellard, E. Trably, G. Kumar, A comprehensive review on two-stage integrative schemes for the valorization of dark fermentative effluents, Crit. Rev. Biotechnol. 38 (2018) 868–882. https://doi.org/10.1080/07388551.2017.1416578.

[22] A.M. Lopez-Hidalgo, A. Sánchez, A. De León-Rodríguez, Simultaneous production of bioethanol and biohydrogen by Escherichia coli WDHL using wheat straw hydrolysate as substrate, Fuel. 188 (2017) 19–27. https://doi.org/10.1016/j.fuel.2016.10.022.

[23] V.E. Balderas-Hernandez, K.P. Landeros Maldonado, A. Sánchez, A. Smoliński, A. De Leon Rodriguez, Improvement of hydrogen production by metabolic engineering of Escherichia coli: Modification on both the PTS system and central carbon metabolism, Int. J. Hydrogen Energy. (2019) 1–10. https://doi.org/10.1016/j.ijhydene.2019.01.162.

565 [24] C.S. Soo, W.S. Yap, W.M. Hon, L.Y. Phang, Mini review: hydrogen and ethanol co-
566 production from waste materials via microbial fermentation, World J. Microbiol.
567 Biotechnol. 31 (2015) 1475–1488. https://doi.org/10.1007/s11274-015-1902-6.
568 [25] B. Sundara Sekar, E. Seol, S. Park, Co-production of hydrogen and ethanol from
569 glucose in Escherichia coli by activation of pentose-phosphate pathway through
570 deletion of phosphoglucose isomerase (pgi) and overexpression of glucose-6-
571 phosphate dehydrogenase (zwf) and 6-phosphogluconate dehyd, Biotechnol.
572 Biofuels. 10 (2017) 1–12. https://doi.org/10.1186/s13068-017-0768-2.
573 [26] B. Sundara Sekar, E. Seol, S. Mohan Raj, S. Park, Co-production of hydrogen and
574 ethanol by pfkA-deficient Escherichia coli with activated pentose-phosphate
575 pathway: Reduction of pyruvate accumulation, Biotechnol. Biofuels. 9 (2016) 1–11.
576 https://doi.org/10.1186/s13068-016-0510-5.
577 [27] A. Sanchez, J.C. Gil, O.A. Rojas-Rejón, A.P. De Alba, A. Medina, R. Flores, R.
578 Puente, Sequential pretreatment strategies under mild conditions for efficient
579 enzymatic hydrolysis of wheat straw, Bioprocess Biosyst. Eng. 38 (2015) 1127–
580 1141. https://doi.org/10.1007/s00449-015-1355-1.
581 [28] P. Sivagurunathan, G. Kumar, A. Mudhoo, E.R. Rene, G.D. Saratale, T. Kobayashi,
582 K. Xu, S.H. Kim, D.H. Kim, Fermentative hydrogen production using lignocellulose
583 biomass: An overview of pre-treatment methods, inhibitor effects and detoxification
584 experiences, Renew. Sustain. Energy Rev. 77 (2017) 28–42.
585 https://doi.org/10.1016/j.rser.2017.03.091.
586 [29] G. Kumar, S. Shobana, D. Nagarajan, D.J. Lee, K.S. Lee, C.Y. Lin, C.Y. Chen, J.S.
587 Chang, Biomass based hydrogen production by dark fermentation — recent trends
588 and opportunities for greener processes, Curr. Opin. Biotechnol. 50 (2018) 136–145.

https://doi.org/10.1016/j.copbio.2017.12.024.

[30] A. Sanchez, G. Magaña, D. Gomez, M. Solís, R. Banares-Alcantara, Bidimensional sustainability analysis of lignocellulosic ethanol production processes. Method and case study, Biofuels, Bioprod. Biorefining. 8 (2014) 670–685. https://doi.org/10.1002/bbb.

[31] A. Sluiter, B. Hames, R.O. Ruiz, C. Scarlata, J. Sluiter, D. Templeton, Determination of Structural Carbohydrates and Lignin in Biomass: Laboratory Analytical Procedure, 2011. https://doi.org/NREL/TP-510-42618.

[32] A.M. Lopez-Hidalgo, A. De Leon-Rodriguez, The Biorefinery Concept: Production of Bioactive Compounds and Biofuels, The Institute for Scientific and Technological Research of San Luis Potosi, 2018. https://repositorio.ipicyt.edu.mx/handle/11627/3153.

[33] G. Davila-Vazquez, A. de León-Rodríguez, F. Alatriste-Mondragón, E. Razo-Flores, The buffer composition impacts the hydrogen production and the microbial community composition in non-axenic cultures, Biomass and Bioenergy. 35 (2011) 3174–3181. https://doi.org/10.1016/j.biombioe.2011.04.046.

[34] L.M. Rosales-Colunga, E. Razo-Flores, L.G. Ordoñez, F. Alatriste-Mondragón, A. De León-Rodríguez, Hydrogen production by Escherichia coli ΔhycA ΔlacI using cheese whey as substrate, Int. J. Hydrogen Energy. 35 (2010) 491–499. https://doi.org/10.1016/j.ijhydene.2009.10.097.

[35] G.L. Miller, Use of Dinitrosalicylic Acid Reagent for Determination of Reducing Sugar, Anal. Chem. 31 (1959) 426–428. https://doi.org/10.1021/ac60147a030.

[36] A. Sanchez, G. Magaña, M.I. Partida, S. Sanchez, Bi-dimensional sustainability analysis of a multi-feed biorefinery design for biofuels co-production from

lignocellulosic residues and agro-industrial wastes, Chem. Eng. Res. Des. 107 (2016) 195–217. https://doi.org/10.1016/j.cherd.2015.10.041.

[37] I. Intelligen, SuperPro Designer v8.5, Products. (2013). https://www.intelligen.com/superpro_overview.html.

[38] A. Sanchez, S. Sanchez, P. Dueñas, P. Hernandez-Sanchez, Y. Guadalajara, The Role of Sustainability Analysis in the Revalorization of Tequila Residues and Wastes Using Biorefineries, Waste and Biomass Valorization. (2019). https://doi.org/10.1007/s12649-019-00756-0.

[39] A. Sanchez, V. Sevilla-Güitrón, G. Magaña, L. Gutierrez, Parametric analysis of total costs and energy efficiency of 2G enzymatic ethanol production, Fuel. 113 (2013) 165–179. https://doi.org/10.1016/j.fuel.2013.05.034.

[40] W.D. Seider, J.D. Seader, D.R. Lewin, S. Widagdo, Product and Process Design Principles: Synthesis, Analysis and Evaluation, 3rd ed., John Wiley & Sons, Inc, Hoboken, NJ, 2009.

[41] M.G. Patterson, What is energy efficiency? Concepts, indicators and methodological issues, Energy Policy. 24 (1996) 377–390. https://doi.org/10.1016/0301-4215(96)00017-1.

[42] Interagency Working Group on the Social Cost of Greenhouse Gases, technical Support Document: Technical Update of the Social Cost of Carbon for Regulatory Impact Analysis Under Executive Order 12866, 2016. https://www.epa.gov/sites/production/files/2016-12/documents/sc_co2_tsd_august_2016.pdf.

[43] United States Environmental Protection Agency, 2018 SO2 Allowance Auction, Clean Air Mark. (2018). https://www.epa.gov/airmarkets/2018-so2-allowance-

auction.

[44] S. Secretariat of Environment and Natural Resources, Mexican Official Standard NOM-001-SEMARNAT-1996, That establishes the Maximum Allowable Limits of Pollutants in Wastewater Discharges in Water Bodies (in Spanish), Official Gazette of the Federation, Mexico, 2003. https://www.profepa.gob.mx/innovaportal/file/3290/1/nom-001-semarnat-1996.pdf.

[45] C. of Deputies, Federal Rights Law (in Spanish), Official Gazette of the Federation, Mexico, 2016. https://www.gob.mx/cms/uploads/attachment/file/243185/Ley_Federal_de_Derechos.pdf.

[46] P. Tello Espinoza, E. Martínez Arce, D. Daza, M. Soulier Faure, H. Terraza, Regional Evaluation on Urban Solid Waste Management in Latin America and the Caribbean - 2010 Report, 2010. https://publications.iadb.org/en/regional-evaluation-urban-solid-waste-management-latin-america-and-caribbean-2010-report.

[47] R. Gaur, S. Soam, S. Sharma, R.P. Gupta, V.R. Bansal, R. Kumar, D.K. Tuli, Bench scale dilute acid pretreatment optimization for producing fermentable sugars from cotton stalk and physicochemical characterization, Ind. Crops Prod. 83 (2016) 104–112. https://doi.org/10.1016/j.indcrop.2015.11.056.

[48] J.C. Parajó, G. Garrote, J.M. Cruz, H. Dominguez, Production of xylooligosaccharides by autohydrolysis of lignocellulosic materials, Trends Food Sci. Technol. 15 (2004) 115–120. https://doi.org/10.1016/j.tifs.2003.09.009.

[49] H. Gu, R. An, J. Bao, Pretreatment refining leads to constant particle size distribution of lignocellulose biomass in enzymatic hydrolysis, Chem. Eng. J. 352 (2018) 198–205. https://doi.org/10.1016/j.cej.2018.06.145.

661 [50] L.J. Jönsson, C. Martín, Pretreatment of lignocellulose: Formation of inhibitory by-
662 products and strategies for minimizing their effects, Bioresour. Technol. 199 (2016)
663 103–112. https://doi.org/10.1016/j.biortech.2015.10.009.
664 [51] H. Zabed, J.N. Sahu, A.N. Boyce, G. Faruq, Fuel ethanol production from
665 lignocellulosic biomass: An overview on feedstocks and technological approaches,
666 Renew. Sustain. Energy Rev. 66 (2016) 751–774.
667 https://doi.org/10.1016/j.rser.2016.08.038.
668 [52] L.J. Jönsson, B. Alriksson, N.-O. Nilvebrant, Bioconversion of lignocellulose:
669 inhibitors and detoxification, Biotechnol. Biofuels. 6 (2013).
670 https://doi.org/https://doi.org/10.1186/1754-6834-6-16.
671 [53] C.S. Soo, W.S. Yap, W.M. Hon, N. Ramli, U.K. Md Shah, L.Y. Phang, Co-
672 production of hydrogen and ethanol by Escherichia coli SS1 and its recombinant,
673 Electron. J. Biotechnol. 30 (2017) 64–70. https://doi.org/10.1016/j.ejbt.2017.09.002.
674 [54] E. Seol, B.S. Sekar, S.M. Raj, S. Park, Co-production of hydrogen and ethanol from
675 glucose by modification of glycolytic pathways in Escherichia coli - from Embden-
676 Meyerhof-Parnas pathway to pentose phosphate pathway, Biotechnol. J. 11 (2016)
677 249–256. https://doi.org/10.1002/biot.201400829.
678
679

Figure captions

Graphical abstract

Fig. 1 Biorefinery block diagram. The process inputs are indicated in blue arrows, and the outputs are marked in green arrows

Fig. 2 Effect of the pretreatment method of lignocellulosic biomass in co-production of hydrogen and ethanol by EtOH-H_2-coproducing *E. coli*. Batch cultures of 0.01L were performed at 31°C and initial pH 8.2 using WSP, WSC, CSP and CSC as substrates. Production and production rate of hydrogen (A), hydrogen yield and TRS consumption (B), production and yield of ethanol (C). Data are presented as mean ± standard deviation

Fig. 3 Kinetics of hydrogen production. Batch cultures (0.01 L) at 31°C and initial pH 8.2 using WSP (A), WSC (B), CSP (C) and CSC (D) as substrates. Data are presented as mean ± standard deviation

Fig. 4 Mass balance for biorefining stages in DAP biorefineries (WSB1 and CSB1)

Fig. 5 Mass balance for biorefining stages in AH-VDAP biorefineries (WSB2 and CSB2)

Fig. 6 Total equipment investment (A) and equipment investment contributions by stage (B) for all biorefineries schemes

Fig. 7 Technoeconomic analysis results. *TPC* and ethanol production (A), *TPC* contributions (B)

Fig. 8 Electricity in-out, electrical productivity and *ERR* for all biorefinery designs

Fig. 9 Indicator analysis for the environmental domain

Fig. 10 Indicator analysis for the economic domain

Fig. 11 Sustainability global values for each biorefinery design

712 **Table 1** Characterization of the hemicellulosic hydrolysates

					Composition (g/L)					
Hydrolysate	Feedstock	Feedstock cost (USD/kg)	Pretreatment	$X_{Hemic.\rightarrow Pentoses}$ (%)	Glucose	Xylose	Arabinose	Formate	Acetate	Furfural
WSC	Wheat straw	$0.08	DAP	88	5.5	29	6.8	1.8	4.2	ND
WSP			AH-VDAP	90	1.8	39.8	7.9	2.6	7.8	1.2
CSC	Corn stover	$0.03	DAP	95	4.7	34.3	9.4	1.2	4.1	ND
CSP			AH-VDAP	95	1.5	41.1	11.3	3.3	4.2	0.8

713 DAP: Diluted acid pretreatment; AH-VDAP: Autohydrolysis followed by very-diluted acid pretreatment; $X_{Hemic.\rightarrow Pentoses}$: Hemicellulose to pentoses mass-
714 conversion; ND: No determinate
715

716 **Table 2** Sustainability framework

Domain	Indicator	Metric, units	Dimensional function	Reference
Environmental	*Emitted GHG (EGHG)*	M_{CO_2}, gCO_{2eq}/MJ_{out}	$M_{CO_2}\cdot C_{CO_2}$	[42]
	Emitted non-GHG (NGHG)	M_{SO_2}, gSO_{2eq}/MJ_{out}	$M_{SO_2}\cdot C_{SO_2}$	[43]
	Water consumption (WCo)	M_{fw}, $L_{fresh\ water}/MJ_{out}$	$M_{fw}\cdot C_{fw}$	[44,45]
		M_{dw}, $L_{discharged\ water}/MJ_{out}$	$M_{dw}\cdot C_{dw}$	
	Wastewater quality (WWQ)	M_{COD}, mg_{COD}/L_{water}	$M_{COD}\cdot C_{COD}$	
		M_{dp}, $kg_{disolved\ pollutants}/MJ_{out}$	$M_{dp}\cdot C_{dp}$	
		T, °C	-	-
		pH	-	-
	Amount of produced solid wastes (SW)	M_{sw}, $kg_{disposable\ wastes}/MJ_{out}$	$M_{sw}\cdot C_{ws}$	[46]
	End Use Energy ratio (*EER*)	M_{EER}, MJ_{out}/MJ_{in}	$(M_{EER}\text{-}1)\cdot C_{TPC}$	-
Economic	*Total production cost* (*TPC*)	M_{TPC}, USD/L_{EtOH}	$M_{TPC}\cdot C_{TEP}$	-
	Electrical productivity (E)	M_E, $Electricity_{out}/Electricity_{in}$	$(M_E\text{-}1)\cdot C_E$	[37]

717 C_{TEP}: Total energy produced; C_E: Cost per MJ of electricity produced as a fraction of total energy produced by
718 the biorefinery
719

720 **Table 3** Metric values for WSB1, WSB2, CSB1 and CSB2 biorefineries and monetizing coefficients for translating metric units to monetized
721 indicators (USD/MJ_{out})

Indicator	Metric	Metric value (M_i)				Monetizing coefficient (C_i)				Monetized metric value ($\eta_i = M_i \cdot C_i$; USD/MJ_{out})				Metric contributions (%)			
		WSB1	WSB2	CSB1	CSB2	WSB1	WSB2	CSB1	CSB2	WSB1	WSB2	CSB1	CSB2	WSB1	WSB2	CSB1	CSB2
EGHG	M_{CO2}	80.70	80.16	101.11	98.76		-1.23E-04			-9.93E-03	-9.86E-03	-1.24E-02	-1.21E-02	16.72	20.86	15.55	17.37
NGHG	M_{SO2}	9.14	8.40	7.29	6.55		-6.00E-08			-5.48E-07	-5.04E-07	-4.38E-07	-3.93E-07	0.00	0.00	0.00	0.00
WCo	M_{fw}	1.40	1.57	1.77	1.95		-1.01E-03			-1.41E-03	-1.58E-03	-1.78E-03	-1.97E-03	2.38	3.34	2.23	2.81
	M_{dw}	0.84	1.14	1.09	1.45		-2.38E-04			-2.00E-04	-2.71E-04	-2.60E-04	-3.46E-04	0.34	0.57	0.33	0.49
WWQ	M_{COD}	129.99	115.45	99.46	91.63	-2.06E-05	-2.78E-05	-2.79E-05	-3.68E-05	-2.68E-03	-3.21E-03	-2.77E-03	-3.37E-03	4.52	6.80	3.47	4.82
	M_{dp}	5.16E-10	4.53E-10	4.31E-10	3.92E-10		-1.40E-04			-7.22E-14	-6.34E-14	-6.04E-14	-5.49E-14	0.00	0.00	0.00	0.00
	T	32.58	31.56	33.01	31.95		0			0.00	0.00	0.00	0.00	0.00	0.00	0.00	0.00
	pH	7	7	7	7		0			0.00	0.00	0.00	0.00	0.00	0.00	0.00	0.00
SW	M_{sw}	3.00E-02	3.31E-03	2.78E-02	6.54E-03		-7.40E-02			-2.22E-03	-2.45E-04	-2.06E-03	-4.84E-04	3.75	0.52	2.58	0.69
ERR	M_{EER}	0.44	0.49	0.33	0.29	-7.61E-02	-6.30E-02	-9.00E-02	-7.29E-02	-4.29E-02	-3.21E-02	-6.07E-02	-5.16E-02	72.29	67.90	75.85	73.81
							Total Environmental Indicator			-0.059	-0.047	-0.080	-0.070				
TPC	M_{TPC}	1.61	1.37	1.96	1.59	-4.72E-02	-4.61E-02	-4.60E-02	-4.60E-02	-7.61E-02	-6.299E-02	-9.01E-02	-7.29E-02	99.26	99.16	98.97	98.81
E	M_E	0.21	0.17	0.33	0.30	-2.75E-03	-3.07E-03	-2.81E-03	-2.93E-03	-5.69E-04	-5.32E-04	-9.33E-04	-8.81E-04	0.74	0.84	1.03	1.19
								Total Economic Indicator		-0.077	-0.064	-0.091	-0.074				
									Global Sustainability Indicator	-0.136	-0.111	-0.171	-0.144				

722

723

724

Table 4 Comparison of hydrogen and ethanol yields obtained by genetically engineered *Escherichia coli* strains

Strain	Genotype description	Substrate	Hydrogen Yield (mL H_2/g substrate)	Ethanol yield (g EtOH/g substrate)	Reference
SH9*_ZG	*E. coli* BW25113 Δ*hycA* Δ*hyaAB* Δ*hybBC* Δ*ldhA* Δ*frdAB* Δ*pfkA*/pEcZG (pDK7 carrying *zwf*, and *gnd*)	Glucose (Glc)	265.6‡ (1.8 mol H_2/mol Glc)	0.36‡ (1.4 mol EtOH/mol Glc)	[26]
SH5 Δ*pgi_Z$_L$G$_G$*	*E. coli* BW25113 Δ*hycA* Δ*hyaAB* Δ*hybBC* Δ*ldhA* Δ*frdAB* Δ*pgi*/pLmZ-GoG (pDK7 carrying *zwf* of *E. coli* BW25113 and *gnd* of *G. oxydans*)		245.8‡ (1.74 mol H_2/mol Glc)	0.41‡ (1.62 mol EtOH/mol Glc)	[25]
SS1-Recombinant *hybC*	*E. coli* SS1/pETDuet-1 (carrying *hybC*)		94.6‡ (0.67 mol H_2/mol Glc)	0.15‡ (0.58 mol EtOH/mol Glc)	[53]
SH8*_ZG	*E. coli* BW25113 Δ*hycA* Δ*hyaAB* Δ*hybBC* Δ*ldhA* Δ*frdAB* Δ*pfkA* Δ*pta-ackA*-adaptive evolution /pEcG (pDK7 carrying *gnd*)		186.5‡ (1.32 mol H_2/mol Glc)	0.35‡ (1.38 mol EtOH/mol Glc)	[54]
WDHL	*E. coli* W3110 Δ*hycA* Δ*lacI*	Wheat straw hydrolysate	159.3	0.32	[22]
WDHGFA	*E. coli* W3110 Δ*hycA* Δ*ptsG* Δ*frdD* Δ*ldhA*		160‡ (0.24 mol H_2/C-mol)	0.26‡ (0.195 mol EtOH/C-mol)	[23]
Ethanol- H_2-coproducing *E. coli*	*E. coli* W3110 Δ*hycA* Δ*ldhA* Δ*frdD*	WSC	311.5	0.33	This work
		WSP	323.1	0.32	
		CSC	312.3	0.34	
		CSP	337.1	0.34	

‡Converted units from the original data (reported units)

728 **Table 5** Pentoses, hydrogen and ethanol production during dark fermentation and alcoholic
729 fermentation stages in all biorefineries schemes

Biorefinery		WSB1	WSB2	CSB1	CSB2
Pretreatment stage	Pentoses (kg/h)	3,673	3,746	4,825	4,912
Dark fermentation stage	$X_{Sugars \rightarrow H_2}$ (%)	14.6	15.1	19.9	21.5
	H_2 (kg/h)	26.3	25.1	44.1	45.8
	$X_{Sugars \rightarrow EtOH}$ (%)	75.0	75.0	66.0	66.0
	EtOH (kg/h)	1,542	1,421	1,677	1,609
Alcoholic fermentation stage	EtOH (kg/h)	4,752	4,923	4,254	4,381
Ethanol production	EtOH (kg/h)	6,093	6,126	5,742	5,796

730 $X_{Sugars \rightarrow H_2}$: Sugars (glucose and pentoses) to hydrogen mass-conversion during dark fermentation stage;
731 $X_{Sugars \rightarrow EtOH}$: Sugars (glucose and pentoses) to ethanol mass-conversion during dark fermentation stage

732

733

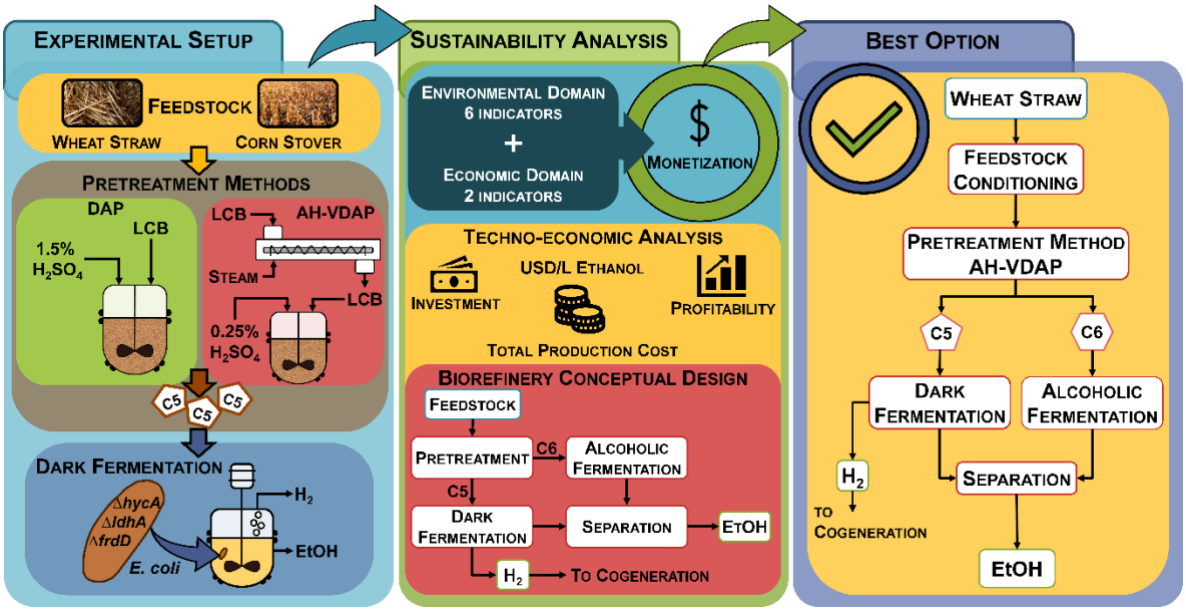

734

735 **Graphical abstract**

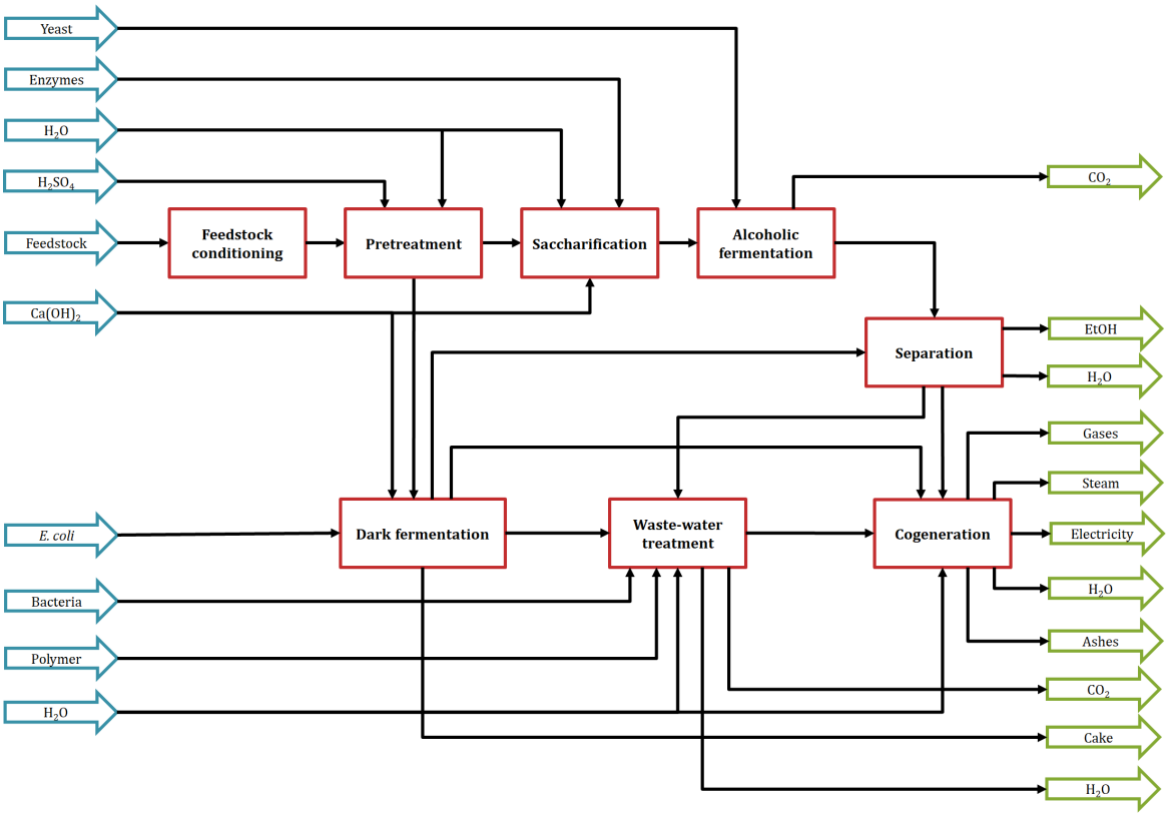
Yeast
Enzymes
H_2O
H_2SO_4
Feedstock
$Ca(OH)_2$
Feedstock conditioning
Pretreatment
Saccharification
Alcoholic fermentation
CO_2
Separation
EtOH
H_2O
Gases
Steam
Electricity
H_2O
Ashes
CO_2
Cake
H_2O
E. coli
Bacteria
Polymer
H_2O
Dark fermentation
Waste-water treatment
Cogeneration

736

737 **Fig. 1**

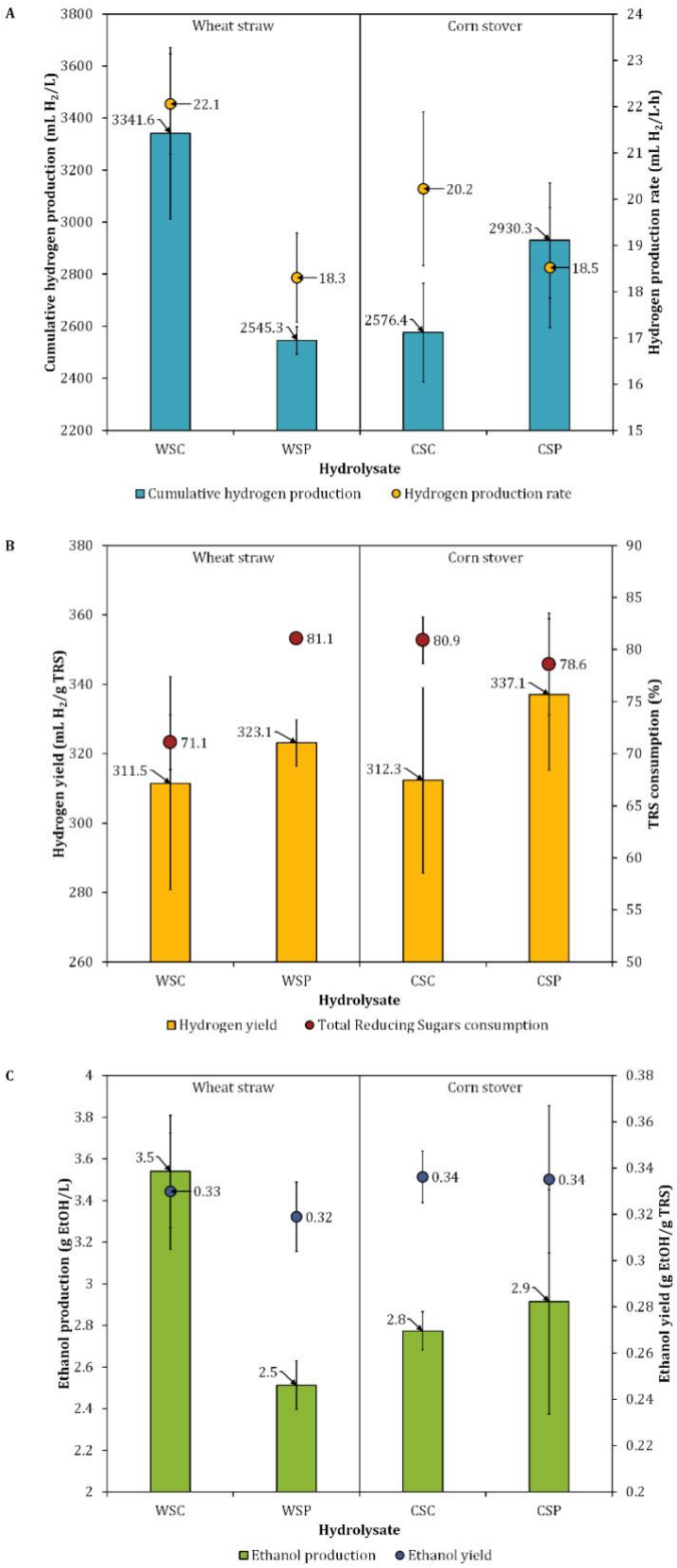
A
Wheat straw
Corn stover
Cumulative hydrogen production (mL H2/L)
Hydrogen production rate (mL H2/L-h)
3341.6
22.1
2545.3
18.3
2576.4
20.2
2930.3
18.5
WSC
WSP
CSC
CSP
Hydrolysate
Cumulative hydrogen production
Hydrogen production rate
B
Wheat straw
Corn stover
Hydrogen yield (mL H2/g TRS)
TRS consumption (%)
311.5
71.1
323.1
81.1
312.3
80.9
337.1
78.6
WSC
WSP
CSC
CSP
Hydrolysate
Hydrogen yield
Total Reducing Sugars consumption
C
Wheat straw
Corn stover
Ethanol production (g EtOH/L)
Ethanol yield (g EtOH/g TRS)
3.5
0.33
2.5
0.32
2.8
0.34
2.9
0.34
WSC
WSP
CSC
CSP
Hydrolysate
Ethanol production
Ethanol yield

Fig. 2

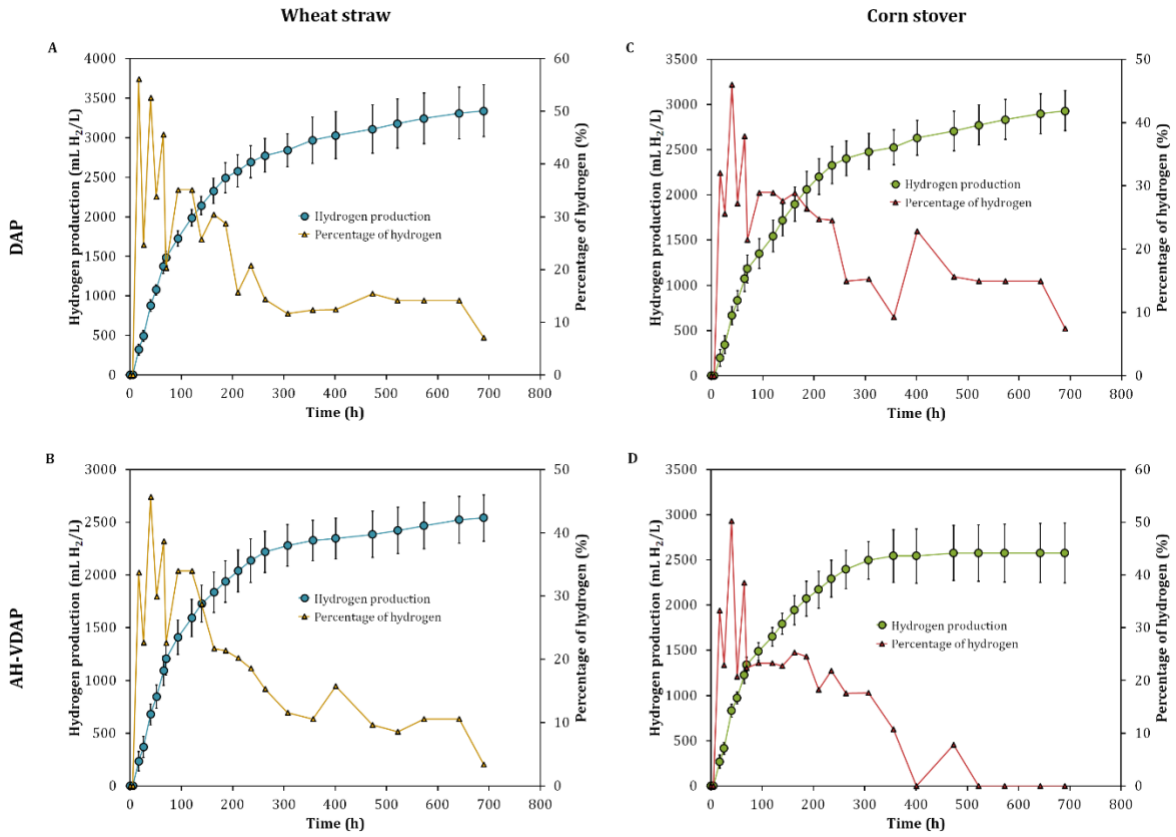
Wheat straw
Corn stover
DAP
AH-VDAP
A
B
C
D
Hydrogen production (mL H2/L)
Percentage of hydrogen (%)
Time (h)
Hydrogen production
Percentage of hydrogen

Fig. 3

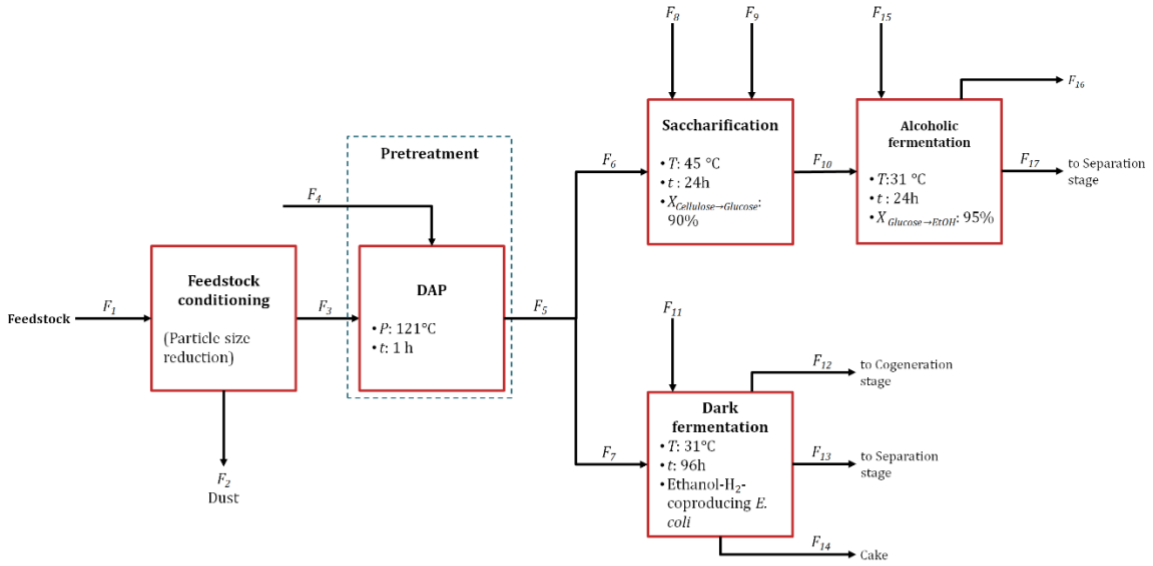

Biorefinery	Feedstock	Stream	F_1	F_2	F_3	F_4	F_5	F_6	F_7	F_8	F_9	F_{10}	F_{11}	F_{12}	F_{13}	F_{14}	F_{15}	F_{16}	F_{17}
WSB1	Wheat straw	Flow (ton/day)	500.0	24.6	475.4	2315.2	2790.5	843.1	1949.9	5.4	1152.0	2003.7	2760.0	42.9	4149.0	471.8	4.4	109.0	1899.2
		Composition (*wt%*)																	
		Cellulose	48.88	9.93	50.90		8.04	26.62				0.27							1.18
		Hemic.	17.83	3.62	18.57		0.38	1.27				0.53							0.56
		Lignig	6.51		6.85		1.17	3.86				1.62							1.71
		H_2O				97.24	80.23	53.11	91.97		100.00	78.80	100.00		98.94	96.62			83.14
		Glucose					0.70	0.23	0.90			11.30			0.04	0.03			0.58
		Xylose					3.16	1.05	4.07			0.44			0.19	0.12			0.04
		EtOH													0.83	0.52			6.01
		H_2												1.47					
		CO_2												98.53				100.00	
		H_2SO_4				2.76	2.29	0.51	3.06										
		Enzyme								100.00		0.27							
		Corn liquor															87.57		
		DAP															12.43		
		NaOAc														2.72			
		Other	26.78	86.45	23.68		4.04	13.36				6.77				0.01			6.78
CSB1	Corn stover	Flow (ton/day)	500.0	3.3	496.8	2315.2	2811.9	842.2	1972.1	4.7	1200.0	2050.2	3960.0	51.1	5693.9	229.5	4.4	97.5	1957.1
		Composition (*wt%*)																	
		Cellulose	43.00	66.04	42.85		7.02	23.44				0.96							1.01
		Hemic.	22.11	33.96	22.03		0.19	0.65				0.27							0.28
		Lignig	18.00		18.12		3.20	10.69				4.39							4.60
		H_2O				97.24	79.49	53.08	90.79		100.00	79.45	100.00		99.06	51.21			83.23
		Glucose					0.61	0.20	0.78			9.71			0.04	0.06			0.49
		Xylose					4.12	1.37	5.28			0.56			0.24	0.42			0.06
		EtOH													0.66	1.16			5.22
		H_2												2.07					
		CO_2												97.93				100.00	
		H_2SO_4				2.76	2.27	0.51	3.02										
		Enzyme								100.00									
		Corn liquor															87.57		
		DAP															12.43		
		NaOAc														9.39			
		Other	16.89		17.00		3.10	10.06	0.13			4.66				37.76			5.11

Fig. 4

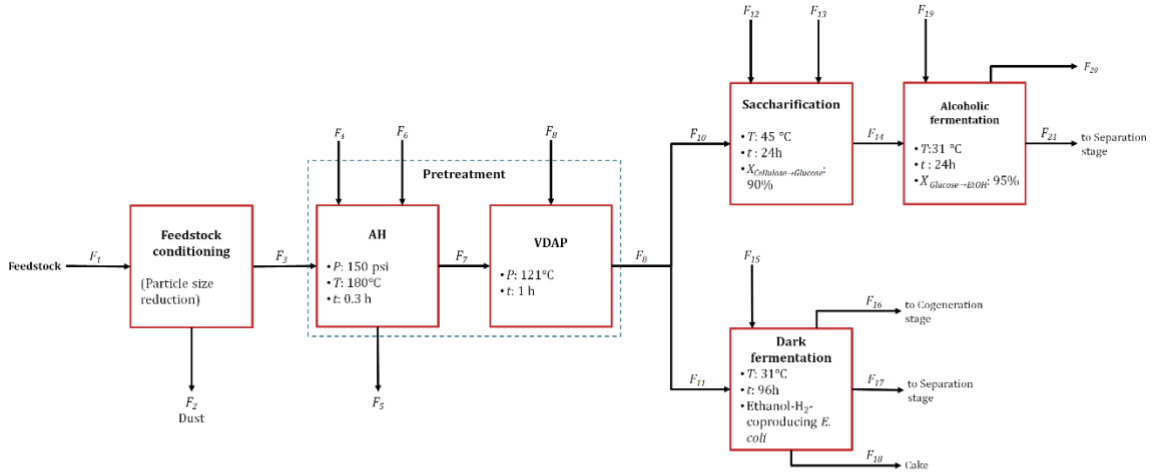

Biorefinery Feedstock		Stream	F_1	F_2	F_3	F_4	F_5	F_6	F_7	F_8	F_9	F_{10}	F_{11}	F_{12}	F_{13}	F_{14}	F_{15}	F_{16}	F_{17}	F_{18}	F_{19}	F_{20}	F_{21}
		Flow (ton/day)	500.0	24.6	475.4	1920.0	1656.0	449.1	1188.4	16.9	1205.3	591.8	615.9	5.7	1397.2	1994.7	3840.0	39.8	3972.4	454.2	4.4	112.9	1886.3
		Composition (*wt%*)																					
		Cellulose	48.88	9.93	50.90				20.36		19.67	40.07				1.19							1.26
		Hemic.	17.83	3.62	18.57				3.07		0.76	1.54				0.46							0.48
		Lignin	6.51		6.85				2.74		2.70	5.50				1.63							1.73
		H_2O				100.00	100.00		59.96	99.54	59.61	32.78	85.55		100.00	78.58	100.00		98.99	96.68			83.10
		Steam						100.00															
		XOS							4.08														
		Glucose									0.45	0.06	0.81			11.91			0.01				0.61
WSB2	Wheat straw	Xylose							0.30		7.46	1.02	13.62			0.30			0.19				0.03
		EtOH																	0.80				6.26
		H_2																1.51					
		CO_2																98.49				100.00	
		H_2SO_4								0.46													
		Enzyme												100.00									
		Corn liquor																			87.57		
		DAP																			12.43		
		NaOAc																		2.70			
		Other	26.78	86.45	23.69				9.48		9.35	19.03	0.01			5.93				0.62			6.53
		Flow (ton/day)	500.0	3.3	496.7	2123.8	1883.8	505.1	1241.9	16.9	1258.7	593.1	668.0	5.0	1365.7	1963.8	5040.0	50.0	5529.3	144.4	4.4	100.4	1867.8
		Composition (*wt%*)																					
		Cellulose	43.00	66.04	42.85				17.14		16.57	35.17				1.06							1.12
		Hemic.	22.11	33.96	22.03				3.97														
		Lignin	18.00		18.12				7.25		7.15	15.17				4.58							4.82
		H_2O				100.00	100.00		59.95	99.54	59.25	33.95	86.63		100.00	78.73	100.00		99.11	77.39			82.78
		Steam						100.00															
		XOS							4.46														
		Glucose									0.38	0.05	0.80			10.64			0.01				0.54
CSB2	Corn stover	Xylose							0.42		9.37	1.33	11.83			0.40			0.23				0.04
		EtOH																	0.65				5.63
		H_2																2.20					
		CO_2																97.80				100.00	
		H_2SO_4								0.46													
		Enzyme												100.00									
		Corn liquor																			87.57		
		DAP																			12.43		
		NaOAc																		15.48			
		Other	16.89		17.00				6.81		7.28	14.33	0.74			4.59				7.13			5.07

Fig. 5

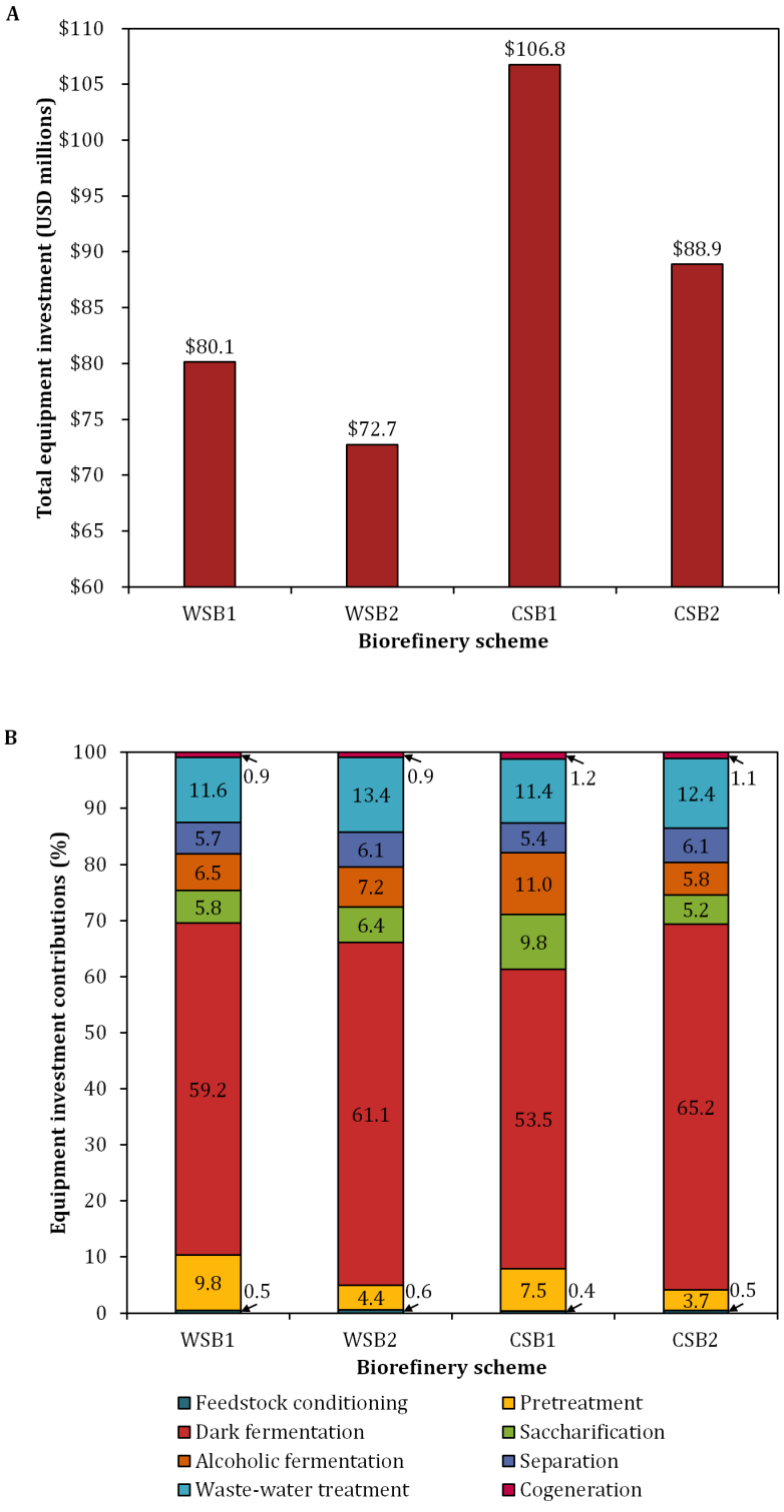

748

749 **Fig. 6**

750

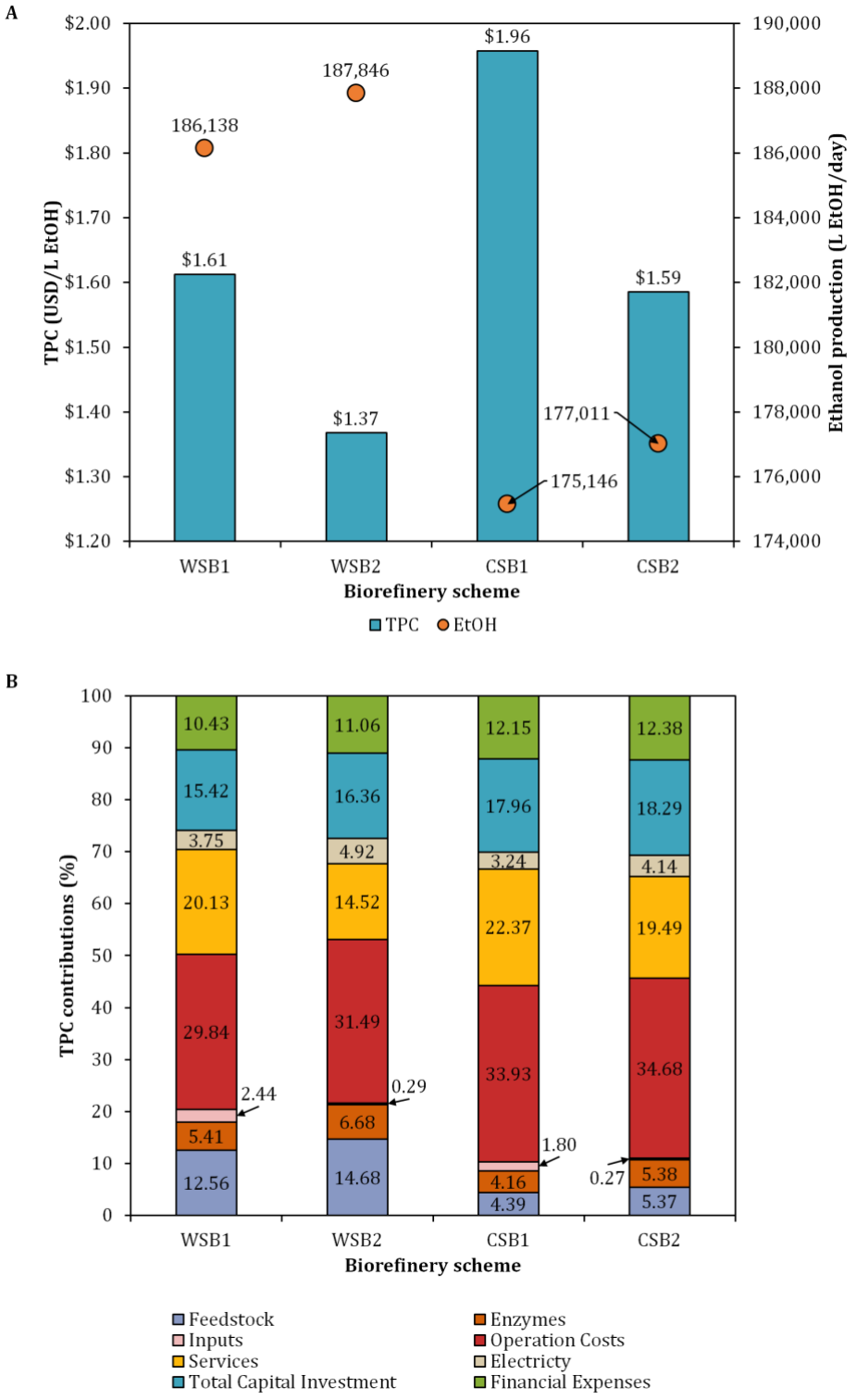
A
$2.00
$1.90
$1.80
$1.70
$1.60
$1.50
$1.40
$1.30
$1.20
TPC (USD/L EtOH)
190,000
188,000
186,000
184,000
182,000
180,000
178,000
176,000
174,000
Ethanol production (L EtOH/day)
$1.61
$1.37
$1.96
$1.59
186,138
187,846
177,011
175,146
WSB1
WSB2
CSB1
CSB2
Biorefinery scheme
TPC
EtOH
B
TPC contributions (%)
100
90
80
70
60
50
40
30
20
10
0
10.43
15.42
3.75
20.13
29.84
2.44
5.41
12.56
11.06
16.36
4.92
14.52
31.49
0.29
6.68
14.68
12.15
17.96
3.24
22.37
33.93
1.80
4.16
4.39
12.38
18.29
4.14
19.49
34.68
0.27
5.38
5.37
WSB1
WSB2
CSB1
CSB2
Biorefinery scheme
Feedstock
Inputs
Services
Total Capital Investment
Enzymes
Operation Costs
Electricty
Financial Expenses

Fig. 7

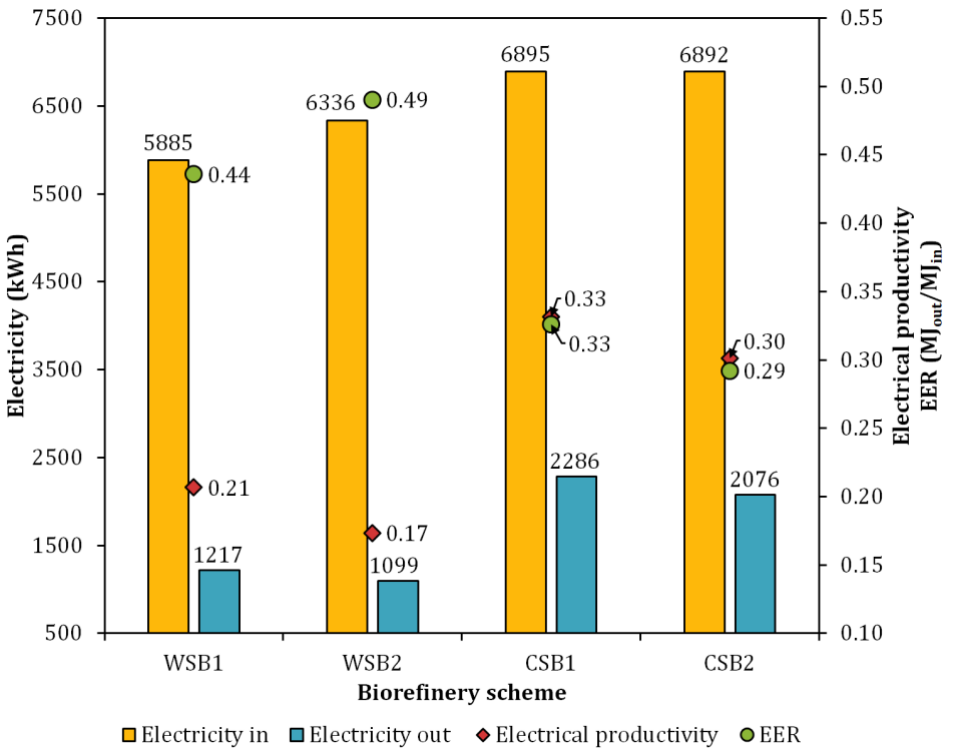

754

755 **Fig. 8**

756

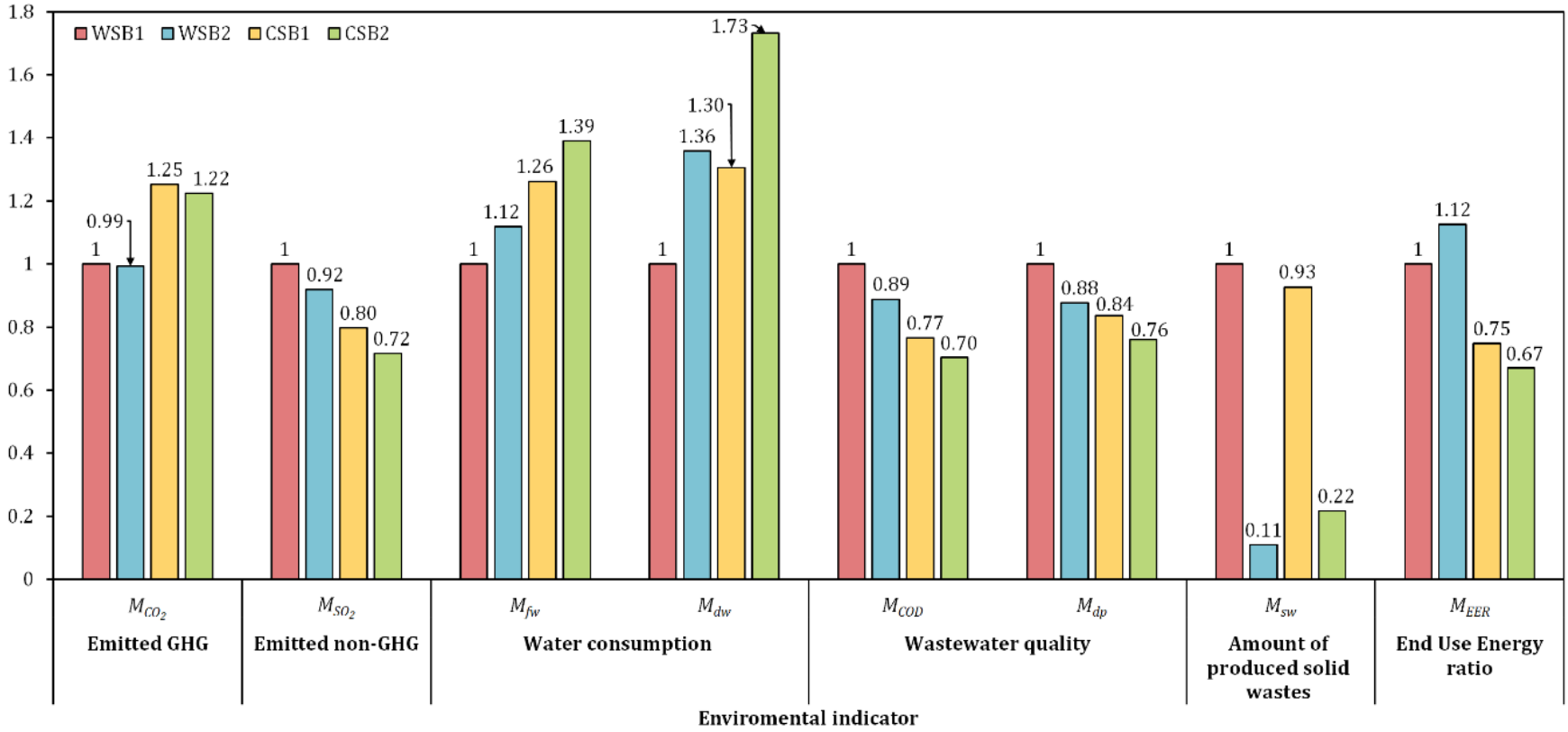
WSB1
WSB2
CSB1
CSB2
1.8
1.6
1.4
1.2
1
0.8
0.6
0.4
0.2
0
1
0.99
1.25
1.22
1
0.92
0.80
0.72
1
1.12
1.26
1.39
1
1.36
1.30
1.73
1
0.89
0.77
0.70
1
0.88
0.84
0.76
1
0.11
0.93
0.22
1
1.12
0.75
0.67
M_{CO_2}
Emitted GHG
M_{SO_2}
Emitted non-GHG
M_{fw}
M_{dw}
Water consumption
M_{COD}
M_{dp}
Wastewater quality
M_{sw}
Amount of produced solid wastes
M_{EER}
End Use Energy ratio
Enviromental indicator

Fig. 9

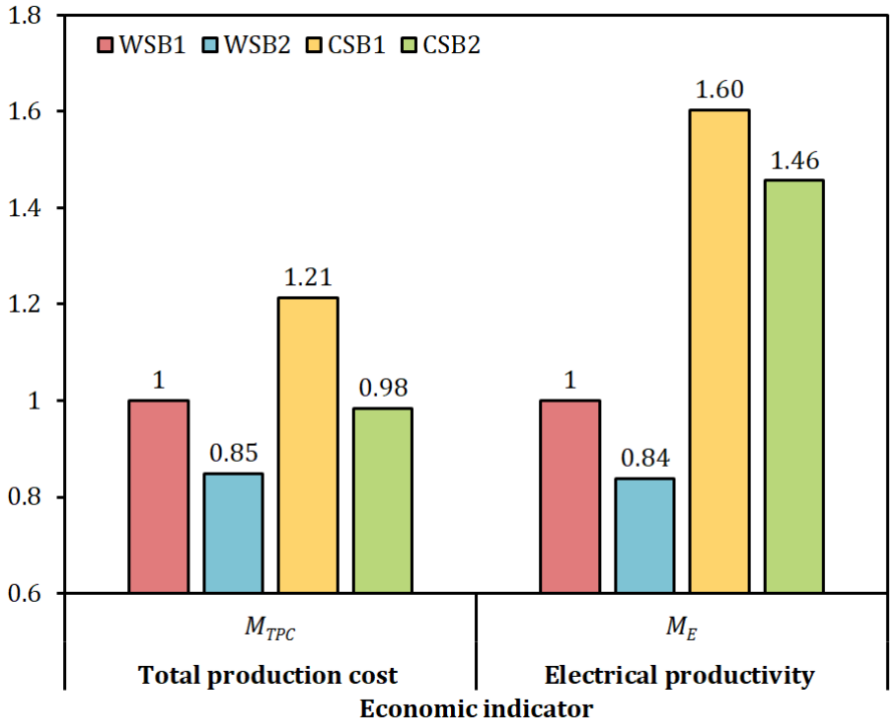

760

761 **Fig. 10**

762

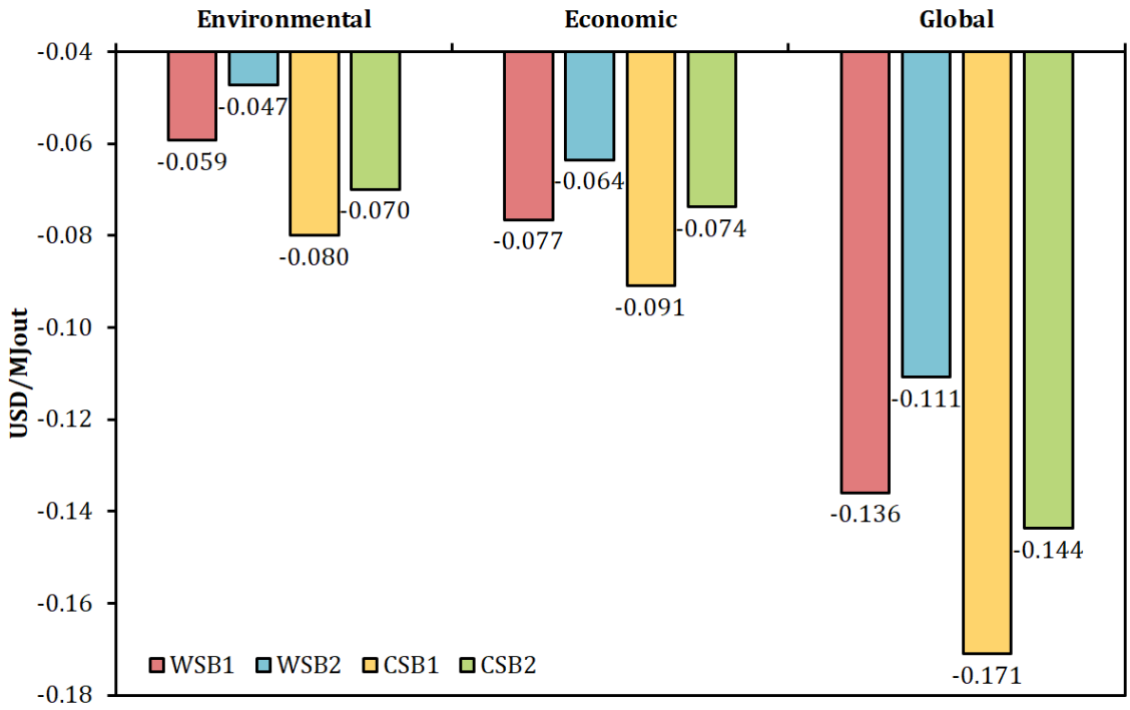

763

764 **Fig. 11**